

## HYDROTHERMAL SYNTHESIS AND CHARACTERIZATION OF COBALT CLAYS

LINDA A. BRUCE, JOHN V. SANDERS, AND TERENCE W. TURNEY

CSIRO, Division of Materials Science, Normamby Road, Clayton, Victoria 3168, Australia

**Abstract**—Reaction of mixtures of cobalt nitrate, colloidal silica, and a metal hydroxide (MOH) under hydrothermal conditions produced a range of cobalt hydroxysilicates, the components of which depended upon the identity of M, temperature, and reactant ratios. At 250°C, if M = Na, a smectite of composition  $\text{Na}_{0.06}\text{Co}_{3.07}\text{Si}_{3.95}\text{O}_{10}(\text{OH})_2$  (I) was produced. If M = K, either a mica,  $\text{KCo}_{2.5}\text{Si}_4\text{O}_{10}(\text{OH})_2$  (II), intermediate between di- and trioctahedral, or a Si-deficient mica,  $\text{KCo}_3\text{Si}_{3.75}\text{O}_{10}(\text{OH})_2$  (III), was formed depending upon the reactant ratios. Similarly, if M = Cs, either a vermiculite or a 2:1 layer silicate intermediate between a mica and a brittle mica was produced. If M = Li, only the non-clay mineral  $\text{Li}_2\text{CoSiO}_4$  was formed. Tetraalkylammonium hydroxides ( $\text{NR}_4\text{OH}$ , R = methyl, ethyl, or propyl) yielded chrysotile. All phases were characterized by elemental analysis, transmission electron microscopy, and X-ray powder diffraction. Further characterization of smectite I was undertaken by diffuse reflectance, infrared, and X-ray photoelectron spectroscopy. The layer charge in these clays appears to stem from cation vacancies within an almost trioctahedral sheet and, possibly, within the tetrahedral sheets. Some of the cobalt present had tetrahedral coordination geometry, but its location was not determined.

**Key Words**—Chrysotile, Cobalt, Mica, Smectite, Synthesis, Talc, Tetraalkylammonium ion, Vermiculite.

### INTRODUCTION

The commercial and geological importance of hydroxysilicates of Mg, Al, and Ca has resulted in extensive studies of their formation under hydrothermal conditions. With the exception of the iron system, corresponding hydrothermal studies of transition-element hydroxysilicates are, at best, fragmentary. As part of a study of the dispersion of metal catalysts on oxide supports, we have examined the interaction of  $\text{Co}^{2+}$  salts with silica in the presence of various alkali metal hydroxides under relatively mild ( $< 300^\circ\text{C}$ ) hydrothermal conditions. Supported cobalt catalysts are of interest in the reduction of carbon monoxide, i.e., The Fischer-Tropsch reaction (see, e.g., Anderson, 1984). Bruce *et al.* (1984) showed that certain cobalt clays are catalytically active under the appropriate conditions; we report here the preparation of some structurally related clay products.

Previous work on the hydrothermal synthesis of cobalt hydroxysilicates has been confined to the following phases: (1) cobalt chrysotile (Noll *et al.*, 1960), (2) cobalt antigorite (Feitnecht and Berger, 1942; Longuet, 1947; Dalmon and Martin, 1968; Dalmon *et al.*, 1973), (3) cobalt kerolite (Pistorius, 1960), (4) cobalt talc (Pistorius, 1960; Dalmon *et al.*, 1968, 1973; De Vynck, 1980), (5) cobalt-mica and hydromica (illite) (De Vynck, 1980), and (6) cobalt amphibole (Gier *et al.*, 1964; Nesterchuk *et al.*, 1968). Brief mention of a cobalt smectite was made by Decarreau (1981).

### EXPERIMENTAL

#### Syntheses

Reactions were performed in unlined static autoclaves (Parr model 4740, 316SS, 71-ml capacity). The colloidal silica

(Snowtex 40, Nissan Chemical Industries Limited) used in this work contained 40.3%  $\text{SiO}_2$ , 0.63%  $\text{Na}_2\text{O}$ , and 0.093%  $\text{Al}_2\text{O}_3$ . All other reagents were A.R. grade. In a typical experiment for the synthesis of NaCo-smectite, a "sodium silicate" solution was freshly prepared by adding colloidal silica (12.00 g, 80 mmole) to a solution of sodium hydroxide (9.60 g, 240 mmole) in water (10 ml) at  $90^\circ\text{C}$ . This solution was added in one portion to  $\text{Co}(\text{NO}_3)_2 \cdot 6\text{H}_2\text{O}$  (14.55 g, 50 mmole) dissolved in hot water (15 ml) and stirred vigorously. The resultant exothermic reaction produced a slurry consisting of a blue solid and colorless mother liquor. An autoclave was charged with all of this mixture, sealed, flushed twice with high purity hydrogen (3.4 MPa), and then heated to  $250^\circ\text{C}$  for 16 hr under an initial partial pressure of hydrogen of 3.4 MPa at STP. After the autoclave was cooled, the pressure was 1.4 MPa; hence, part of the hydrogen had been consumed. All gases were vented, and the blue slurry in the autoclave was dispersed in one liter of water. After four centrifugation and washing cycles (total of 4 liters of distilled water), the supernatant liquid had a  $\text{pH} < 8$ . A sample of the blue solid was further purified for elemental analysis by dialysis for one week. Table 1 gives a summary of experimental conditions and the resulting identified phases.

#### Analytical procedures

Solid products were examined by X-ray powder diffraction (XRD) using a Siemens D-500 diffractometer with Fe-filtered  $\text{CoK}\alpha$  radiation. When necessary, samples were kept wet by wrapping the Perspex sample holder in a polyethylene film. No special precautions were taken to control the atmosphere for dry samples.

For electron microscopy (TEM), the synthetic products were dispersed ultrasonically in alcohol and samples were collected on holey carbon films and examined in a JEOL 100 CX electron microscope (objective lens  $C_s = 0.7$  mm) fitted with a top-entry, double-tilting stage. Morphologically different phases were identified by selected area electron diffraction (SAD).

Infrared (IR) spectra were recorded on a Pye-Unicam SP3-300 spectrophotometer from KBr discs (0.2–2 mg sample/100 mg KBr), dried at  $130^\circ\text{C}$  for 24 hr. Diffuse reflectance

Table 1. Summary of hydrothermal experiments.

| Reactant stoichiometry <sup>1</sup> |    |     | Conditions <sup>2</sup>   | Phases identified <sup>3</sup>   |
|-------------------------------------|----|-----|---|--|
| Co                                  | Si | OH  |   |  |
| <b>Lithium</b>                      |    |     |   |  |
| 25                                  | 40 | 120 |   | $\beta_{II}$ - and $\gamma_{II}$ -Li <sub>2</sub> CoSiO <sub>4</sub>                   |
| <b>Sodium</b>                       |    |     |   |  |
| 25                                  | 40 | 120 |   | NaCo-smectite, trace Na <sub>2</sub> CoSiO <sub>4</sub>                                |
| 25                                  | 40 | 120 | no H <sub>2</sub>   | Co <sub>3</sub> O <sub>4</sub> , some NaCo-smectite                                    |
| 25                                  | 40 | 120 | 300°C   | Co <sub>3</sub> O <sub>4</sub> , NaCo-smectite   |
| 25                                  | 40 | 120 | H <sub>2</sub> (30 MPa)   | NaCo-smectite, some Co metal   |
| 25                                  | 40 | 500 |   | Na <sub>2</sub> CoSiO <sub>4</sub> , $\beta$ -Co(OH) <sub>2</sub> <sup>4</sup>         |
| 25                                  | 40 | 60  |   | "Crumpled foil" phase  |
| 25                                  | 40 | 120 | no H <sub>2</sub> , 150°C   | "Crumpled foil," some NaCo-smectite  |
| 60                                  | 40 | 100 |   | NaCo-smectite, Co <sub>3</sub> O <sub>4</sub> , Co metal                               |
| 25                                  | 70 | 120 |   | NaCo-smectite, noncrystalline silica   |
| 25                                  | 40 | 140 | H <sub>2</sub> (0.7 MPa), 350°<br>NaOH (40) NMe <sub>4</sub> OH (100) | Co-talc, some "crumpled foil" <sup>5</sup>   |
| 25                                  | 40 | 120 | NEt <sub>4</sub> Br (160) added                                       | "Crumpled foil," trace Co-chrysotile <sup>5</sup>                                      |
| <b>Potassium</b>                    |    |     |   |  |
| 25                                  | 40 | 120 |   | KCo-mica (Co deficient)  |
| 30                                  | 20 | 120 |   | KCo-micas (Si deficient and Co deficient), $\alpha$ - and $\beta$ -Co(OH) <sub>2</sub> |
| <b>Cesium</b>                       |    |     |   |  |
| 30                                  | 20 | 100 |   | CsCo-brittle mica, some $\beta$ -Co(OH) <sub>2</sub>                                   |
| 25                                  | 40 | 120 |   | CsCo-vermiculite   |
| <b>Tetraethylammonium</b>           |    |     |   |  |
| 30                                  | 20 | 150 |   | Co-chrysotile, trace "crumpled foil" <sup>5</sup>                                      |
| 25                                  | 40 | 120 | N(CH <sub>3</sub> ) <sub>4</sub> OH used                              | "Crumpled foil," hexagonal plates <sup>6</sup>   |
| 30                                  | 20 | 50  | NaCl (50) added   | "Crumpled foil," noncrystalline SiO <sub>2</sub> <sup>6</sup>                          |

<sup>1</sup> Millimoles of reactants used, cobalt added as the nitrate, silicon as 40% w/w colloidal silica.

<sup>2</sup> All reactions were performed at 250°C for 16 hr under an initial pressure of hydrogen (3.4 MPa at STP), unless stated otherwise.

<sup>3</sup> Identification was by X-ray powder or electron diffraction and by transmission electron microscopy.

<sup>4</sup> Soluble anion [Co(OH)<sub>4</sub>]<sup>-</sup> was also produced.

<sup>5</sup> Extensive thermolysis of the tetraethylammonium ion occurred. Products identified by gas chromatography-mass spectrometry included triethylamine, ethane, ethene, methane, and higher molecular weight hydrocarbons.

<sup>6</sup> Composition of this phase was not determined.

electronic spectra were recorded against BaSO<sub>4</sub> on a Pye-Unicam SP8-100 spectrophotometer using an integrating sphere accessory (Part No. 790825). X-ray photoelectron spectra (XPS) were recorded on a Vacuum Generators' ESCALAB with an aluminum anode at 150 W (pass energy 30 eV, 4-mm slits).

Wet chemical analyses were performed by inductively coupled plasma atomic emission spectroscopy or by atomic absorption spectrophotometry on samples pre-dried at 120°C in vacuum for 6 hr. Analytical data are presented in Table 2. Water loss on ignition could not be determined because of simultaneous and partially reversible oxidation of CoO to Co<sub>3</sub>O<sub>4</sub> during heating. Total elemental analysis was, therefore, not possible.

## RESULTS

### Clay synthesis in the presence of sodium

The slurry derived from admixture of cobalt nitrate, colloidal silica, and sodium hydroxide solutions (molar ratios of Co:Si:OH = 2.5:4:12) was strongly basic, and all of the cobalt precipitated (i.e., the supernatant solution contained neither [Co(H<sub>2</sub>O)<sub>6</sub>]<sup>2+</sup> nor [Co(OH)<sub>4</sub>]<sup>2-</sup> ions). In this solid, the only crystalline phase detectable by XRD was  $\beta$ -Co(OH)<sub>2</sub> (JCPDS #30-443). On heating

this slurry to 250°C for 16 hr under hydrogen pressure, a bright blue flocculent material was obtained as the predominant solid product. The properties of this solid (hereinafter called "NaCo-smectite") are described below. Minor amounts of deep blue, highly crystalline Na<sub>2</sub>CoSiO<sub>4</sub> (JCPDS #25-823) were also detected in some preparations. For reactions performed in the absence of hydrogen or at elevated temperatures (e.g., >300°C) Co<sub>3</sub>O<sub>4</sub> (JCPDS #9-148) was the major product. A hydrogen atmosphere appeared to be necessary to prevent partial oxidation of Co<sup>2+</sup> to Co<sup>3+</sup> by the nitrate counterion present in the reaction medium. Extensive nitrate reduction was evident from the strong odor of ammonia noted when the autoclave was vented. Chemical analysis and XPS indicated that no nitrogen was incorporated, for example, as a cobalt-amine complex, in any of the samples. At excessively high hydrogen partial pressures (>30 MPa) some of the cobalt was reduced to the metal (f.c.c. Co, JCPDS #15-806).

Varying the ratios of reactants or the experimental conditions had a profound effect upon the product.

Table 2. Cation analyses for cobalt clays.

| Compound  | Method <sup>1</sup> | Analysis (wt. %) |                  |           | Formula <sup>2</sup> |      |           |
|---|---------------------|------------------|------------------|-----------|----------------------|------|-----------|
|   |                     | CoO              | SiO <sub>2</sub> | Other     | Co                   | Si   | Other     |
| NaCo-smectite                                   | A <sup>3</sup>      | 29.9             | 39.19            | 0.24 (Na) | 3.07                 | 3.95 | 0.06 (Na) |
|   | A <sup>3</sup>      | 30.1             | 38.74            | 0.30 (Na) | 3.10                 | 3.93 | 0.08 (Na) |
|   | X                   |                  |                  |           | 3.02                 | 3.92 | 0.28 (Na) |
| NaCo-smectite (acid treated)<br>"Crumpled foil" | A                   | 27.8             | 45.3             | 0.11 (Na) | 2.40 <sup>4</sup>    | 3.95 | 0.02 (Na) |
|   | A                   | 25.4             | 47.0             | 2.16 (Na) | 2.32 <sup>5</sup>    | 4.21 | 0.52 (Na) |
| KCo-mica (Si-deficient)                         | X                   |                  |                  |           | 2.59                 | 4.07 | 0.54 (Na) |
|   | X                   |                  |                  |           | 3.00                 | 3.73 | 1.08 (K)  |
| KCo-mica (Co-deficient)                         | A                   | 29.0             | 45.1             | 6.22 (K)  | 2.31                 | 4.12 | 0.90 (K)  |
|   | X                   |                  |                  |           | 2.50                 | 3.98 | 1.08 (K)  |
| CsCo-mica                                       | X                   |                  |                  |           | 3.03                 | 3.65 | 1.34 (Cs) |
| CsCo-vermiculite                                | X                   |                  |                  |           | 3.23                 | 3.71 | 0.70 (Cs) |
| Co-chrysotile                                   | X                   |                  |                  |           | 2.68 <sup>6</sup>    | 2.16 |           |

<sup>1</sup> A = wet chemical analysis; X = X-ray photoelectron spectra.

<sup>2</sup> Formulae based on total cation charge of 22 expected for a 2:1 layer silicate.

<sup>3</sup> Analyses from two different preparations.

<sup>4</sup> Formula based on no loss of Si from original NaCo-smectite.

<sup>5</sup> Formula based on total cation charge of 22.

<sup>6</sup> Formula based on total cation charge of 14 expected for a 1:1 layer silicate.

Thus, in the presence of a large excess of base (Co:Si:OH = 2.5:4:50), the Co(OH)<sub>2</sub> initially present reacted further to produce, in part, deep blue solutions of [Co(OH)<sub>4</sub>]<sup>2-</sup>, whose electronic spectrum [ $\nu_{\max}$  = 535(sh), 590, 620 nm] was close to that published by Cotton *et al.* (1961). A second product was deep blue Na<sub>2</sub>CoSiO<sub>4</sub>; no NaCo-smectite was formed. With a deficiency of base at the same Co/Si ratio (Co:Si:OH = 2.5:4:6), a mauve, poorly ordered solid was produced at 250°C. This material had a flake-like or "crumpled foil" morphology and is structurally related to the smectite phase (*vide infra*). At lower temperatures (150°–200°C), these poorly-ordered phases predominated even at higher base-to-silica ratios.

At 350°C (150 hr) and at a partial pressure of hydrogen of 0.7 MPa a pink talc phase was prepared from a mixture of sodium and tetraethylammonium (TEA) hydroxides (Co:Si:Na:TEA = 2.5:4:2:5). This phase had a basal spacing of 9.55 Å and did not expand upon treatment with ethylene glycol. It was similar to the cobalt talc reported by de Vynck (1980) in morphology, XRD pattern, and infrared spectrum. In systems with high Co/Si ratios (Co:Si:OH = 3:2:12), excess Co was converted primarily into Co<sub>3</sub>O<sub>4</sub> or remained as unreacted β-Co(OH)<sub>2</sub>; NaCo-smectite was the principal silicate present. Similarly, at low Co/Si ratios (Co:Si:OH = 2.5:7:12) the excess of silica remained unchanged in the reaction, and the Co was present in the smectite phase.

Thus, below 250°C, in the presence of NaOH only NaCo-smectite, a related, poorly ordered phase, and Na<sub>2</sub>CoSiO<sub>4</sub> were formed. Decarreau (1981) reported the synthesis of a Co-smectite, formulated as a stevensite [i.e., Na<sub>2x</sub>Co<sub>3-x</sub>(Si<sub>4</sub>O<sub>10</sub>)(OH)<sub>2</sub>], by the reaction of Co<sup>2+</sup> chloride and sodium silicate (2 weeks, 75°C);

however, this material differs in its XRD and electronic spectrum from the NaCo-smectite found in the present study.

#### Characterization of NaCo-smectite and related phases

*X-ray and electron diffraction studies.* XRD patterns of NaCo-smectite products generally showed a strong

Table 3. X-ray powder and selected area diffraction data for NaCo-clays.

| Cobalt smectite                                 |                               |          |       | Indices<br>001 or <i>hk</i> | d <sub>calc</sub> <sup>2</sup><br>(Å) | "Crumpled foils"<br>SAD<br>d (Å) (l) <sup>3</sup> |
|---|-------------------------------|----------|-------|-----------------------------|---------------------------------------|---|
| X-ray <sup>1</sup><br>d (Å) (l/l <sub>0</sub> ) | SAD<br>d (Å) (l) <sup>3</sup> |          |       |                             |                                       |   |
| 12.4 (100)                                      |                               | 001      | 12.35 |                             |                                       |   |
| 6.16 (1)  |                               | 002      | 6.17  |                             |                                       |   |
| 4.61 (5)  | 4.60 (s)                      | 11,02    | 4.63  | 4.60 (s)                    |                                       |   |
| 4.14 (3)  |                               | 003      | 4.12  |                             |                                       |   |
| 3.10 (17)                                       |                               | 004      | 3.09  |                             |                                       |   |
| 2.66 (8)  | 2.69 (s)                      | 20,13    | 2.66  | 2.63 (s)                    |                                       |   |
|   | 2.35 (w)                      | 22,04    | 2.31  | 2.29 (w)                    |                                       |   |
|   | 1.75 (m)                      | 31,24,15 | 1.75  | 1.74 (m)                    |                                       |   |
| 1.553 (8)                                       |                               |          | 1.557 |                             |                                       |   |
|   | 1.55 (vs)                     | 06,33    |       | 1.54 (vs)                   |                                       |   |
| 1.545 (5)                                       |                               |          | 1.543 |                             |                                       |   |
|   | 1.35 (m)                      | 26,07    | 1.344 |                             |                                       |   |
|   | 1.32 (w)                      | 31,32,40 | 1.319 | 1.312 (3)                   |                                       |   |
|   |                               | 42,35    | 1.281 | 1.270 (w)                   |                                       |   |
|   |                               | 18,45    | 1.140 | 1.115 (w)                   |                                       |   |
|   |                               | 51,50,37 | 1.059 | 1.058 (w)                   |                                       |   |
|   |                               | 53,46,19 | 1.908 | 1.001 (m, br)               |                                       |   |
|   |                               | 1,10,55  | 0.920 | 0.918 (w)                   |                                       |   |
|   |                               | 61,60,56 | 0.884 | 0.885 (m)                   |                                       |   |

<sup>1</sup> Air-dried sample.

<sup>2</sup> Based on a monoclinic cell with  $a = 5.37$ ,  $b = 9.34$ ,  $c = 12.44$  Å,  $\beta = 97^\circ$ .

<sup>3</sup> s = strong, m = medium, w = weak, sh = shoulder, br = broad.

Table 4. Effect of treatment on basal spacings in NaCo-smectite.

| Treatment       | Spacing (Å) |
|-----------------|-------------|
| Wet             | 15.2        |
| Air-dried       | 12.4        |
| 120°C           | 10.2        |
| 350°C           | 9.9         |
| 500°C           | 9.8         |
| Ethylene glycol | 16.9        |
| Glycerol        | 17.3        |

basal spacing plus several higher order reflections (Table 3). As expected for a smectite, the magnitude of the 001 spacing was highly dependent upon the degree of hydration, and the layers expanded readily on glycolation (Table 4). Dehydration was partially reversible at temperatures even as high as 500°C.

As a result of preferred orientation of the smectite plates, the two-dimensional *hk* XRD reflections were weak; however, these reflections were readily observed by electron diffraction (Figure 1a, Table 3) and were indexed satisfactorily ( $a = 5.37$ ,  $b = 9.34$  Å). An SAD pattern of a single smectite plate (Figure 2a) clearly showed the hexagonal symmetry expected for a trioctahedral 2:1 layer structure. The absence of *hkl* ( $l \neq 0$ ) reflections was expected for a phyllosilicate whose plates were oriented normal to the electron beam. The value of the 06 reflection (1.557 Å from XRD) was larger than that generally found for a trioctahedral Mg-smectite (*cf.* hectorite 06,33 at 1.530 Å or stevensite at 1.520 Å; Brindley and Brown, 1980). This value may be partly due to the larger ionic radius of high-spin, octahedral  $\text{Co}^{2+}$  (0.754 Å) compared with  $\text{Mg}^{2+}$  (0.720 Å; Shannon, 1976). A similar increase in 06 reflection was found by Hazen and Wones (1972) for Fe-substituted Mg-micas.

Transmission electron micrographs of NaCo-smectite samples show hexagonal plates, generally with rounded corners (Figure 1a). At high resolution, the hexagonal net in the (*hk*) plane is clearly visible, as is the packing of layers to form "books" about 5–20 layers thick (Figure 2).

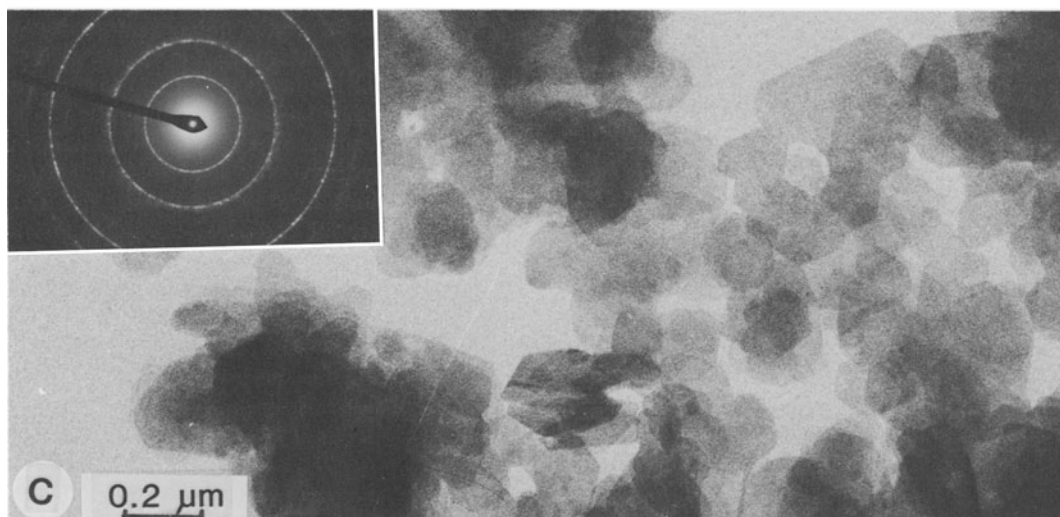
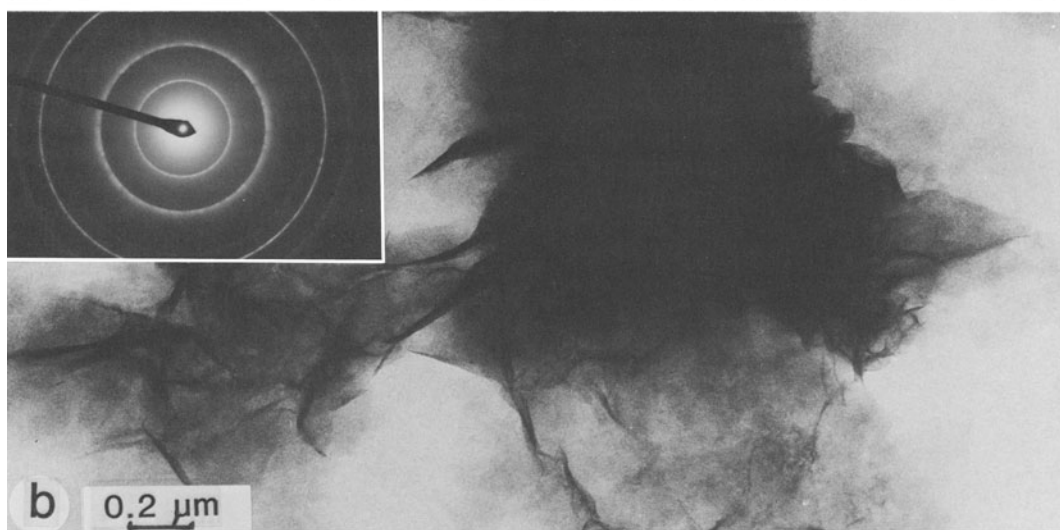
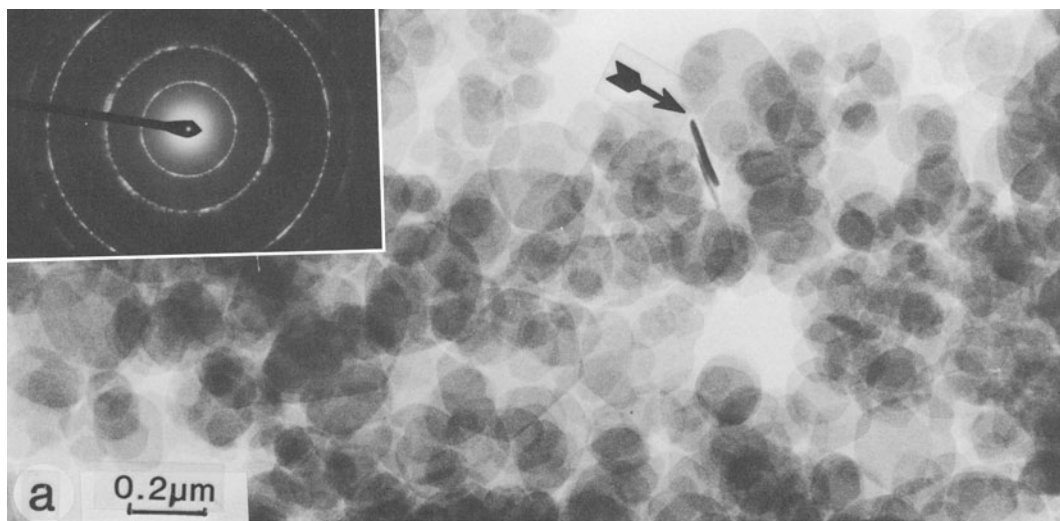
Samples of the "crumpled foil" phase generally exhibited rather featureless XRD patterns, commonly with a broad, weak reflection between 15 and 25 Å and a somewhat sharper reflection at about 1.54 Å. Transmission electron micrographs show a characteristic "crumpled foil" morphology (Figure 1b) together with regions of material with very little contrast. SAD stud-

ies, however, even of areas of poor contrast, showed them to be strongly diffracting and to yield a pattern essentially the same as that of a well-crystalline sample of NaCo-smectite (Table 3). Presumably the crumpled foils contain regions with a two-dimensional layer structure similar to that of the smectite, but structural imperfections within the sheets cause stresses, which lead to a buckling of the layers.

**Chemical analysis.** Based on X-ray and electron diffraction results, the NaCo-smectite phase may be formulated as a 2:1 phyllosilicate. The composition considered in terms of a 2:1 structure requires the sum of the cation charges to be 22 to balance the  $\text{O}_{10}(\text{OH})_2$  unit. Chemical analysis yielded the approximate formula  $\text{Na}_{0.06}\text{Co}_{3.07}\text{Si}_{3.95}\text{O}_{10}(\text{OH})_2 \cdot 6.6 \text{H}_2\text{O}$  for the NaCo-smectite. Compositions from XPS, which showed no other elements to be present in appreciable amounts, were in general agreement, but yielded a somewhat larger value for Na (Table 2). This large value for Na may well be a result of a local concentration of Na on the surface of the clay particles. For the crumpled foil phase, chemical analysis gave an approximate formula  $\text{Na}_{0.52}\text{Co}_{2.32}\text{Si}_{4.21}\text{O}_{10}(\text{OH})_2 \cdot 4 \text{H}_2\text{O}$ , based on 22 as the sum of cation charges. The excess of Si indicated by this formula may well be due to the structural imperfections that caused the buckling noted above. Analysis of a sample of the NaCo-smectite which had been acid washed (ammonium acetate/acetic acid buffered at pH 4) for 1 hr suggested that extensive extraction of cobalt had taken place to give a solid with composition,  $\text{Na}_{0.02}\text{Co}_{2.40}\text{Si}_{3.95}\text{O}_{10}(\text{OH})_{0.62} \cdot 9.5 \text{H}_2\text{O}$ , assuming the same tetrahedral occupancy by Si as in the NaCo-smectite. Even after this mild acid treatment the 2:1 layer structure was retained, as evidenced by the intense 001 spacing at 10.3 Å for a sample dried at 110°C, which changed to two peaks at 12.7 at 15.7 Å upon treatment with water at room temperature.

**Electronic spectra.** The diffuse reflectance, ultraviolet-visible spectrum of the blue NaCo-smectite exhibited bands at  $\nu_{\text{max}}$  18,000(sh), 16,800(sh), and 15,600  $\text{cm}^{-1}$  (Figure 3). This spectrum contrasts with that typically found for regular octahedral, high-spin  $\text{Co}^{2+}$  in which a  ${}^4\text{T}_{1g}(\text{F}) \rightarrow {}^4\text{T}_{1g}(\text{P})$  transition is observed at about 19,000–20,000  $\text{cm}^{-1}$ . Distortion of the octahedral ligand field can split the  ${}^4\text{T}_{1g}(\text{P})$  level and results in a somewhat lower value (e.g., 17,250  $\text{cm}^{-1}$  in  $\text{CoCl}_2$  or 17,500  $\text{cm}^{-1}$  in  $\text{Co}_2\text{SiO}_4$ ; Fergusson, 1970). The position of  $\nu_{\text{max}}$  in NaCo-smectite, however, is typical for high spin cobalt in a tetrahedral field in which an in-

Figure 1. Transmission electron micrograph and diffraction pattern of (a) NaCo-smectite showing rounded thin plates. Thickness ( $\sim 100$  Å) may be measured where they stand parallel to the electron beam (arrowed), (b) "crumpled foil" phase with no visible regular structure. Its diffraction pattern, however, is almost identical to that of the smectite, and (c) Co-talc, also closely resembling the smectite in diffraction pattern and morphology.



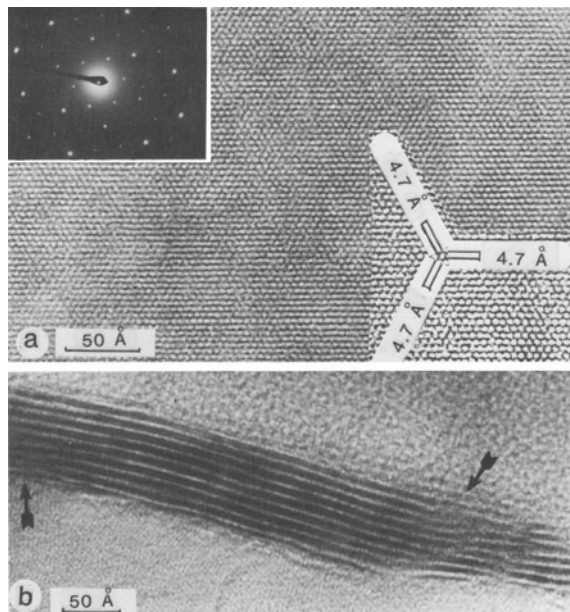


Figure 2. High-resolution transmission electron micrographs of NaCo-smectite (a) lattice images of the [001] projection and diffraction pattern from a single plate showing the hexagonal  $hk0$  net of spots; (b) where the layers stand on end, an interlamellar spacing of about 10 Å can be seen from the fringes. It is not possible to interpret the disorder apparent (arrowed) in these fringes.

tense  ${}^4A_2 \rightarrow {}^4T_1(P)$  transition is usually found in the 14,000–17,000- $\text{cm}^{-1}$  region. It is highly unlikely that distortions of coordination geometry within the octahedral sheet alone could produce such a value. The blue color of the NaCo-smectite contrasts with the pink color of the Co-talc ( $\nu_{\text{max}}$  15,800(sh), 21,000  $\text{cm}^{-1}$ ) and the acid-treated smectite ( $\nu_{\text{max}}$  19,400  $\text{cm}^{-1}$ ), in which cobalt is in a more or less regular octahedral environment.

In view of the similarity to other 2:1 phyllosilicates, most of the cobalt probably resides in an octahedral environment in NaCo-smectite; however, the presence of relatively low concentrations of tetrahedral cobalt would be sufficient to mask the more abundant octahedral form. The visible transition is generally at least an order of magnitude more intense for tetrahedral than for octahedral cobalt (Fergusson, 1970).

**Infrared spectra.** NaCo-smectite contained both structural hydroxyl and interlayer water as can be seen from its IR spectrum (Figure 4a). Two bands at 3620 and 3565  $\text{cm}^{-1}$  are attributable to structural  $\nu(\text{OH})$  and a broader band at 3420  $\text{cm}^{-1}$  to the  $\nu(\text{OH})$  of interlayer water. These vibrations contrast with the poorly ordered “crumpled foil” phase in which only a single  $\nu(\text{OH})$  band was noted at 3625  $\text{cm}^{-1}$ , together with a broader water absorption, and with Co-talc which showed a sharp structural  $\nu(\text{OH})$  band at 3634  $\text{cm}^{-1}$

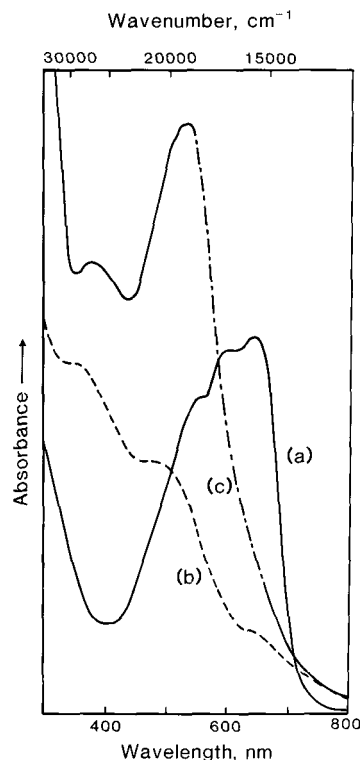


Figure 3. Diffuse reflectance electronic spectra of (a) NaCo-smectite, (b) Co-talc, and (c) acid-washed NaCo-smectite.

and no interlayer water  $\nu(\text{OH})$  band. The acid-treated NaCo-smectite also exhibited two structural  $\nu(\text{OH})$  bands at 3630 and 3560  $\text{cm}^{-1}$ . In similar 2:1 phyllosilicates, the presence of two  $\nu(\text{OH})$  bands rather than one has been ascribed to the existence of two sites of different symmetry involving OH groups close to an octahedral vacancy (Tateyama *et al.*, 1976).

Vibrations in the region 650–950  $\text{cm}^{-1}$  have been used frequently to determine the nature of the octahedral sheet in 2:1 silicates (Farmer, 1974; Brindley *et al.*, 1979). A single band of medium intensity at 660  $\text{cm}^{-1}$  in NaCo-smectite is assigned to a deformation mode of an hydroxyl linked to three cobalt atoms. Similar vibrations are found in Co-talc [ $\delta(\text{Co}_3\text{OH})$  at 662  $\text{cm}^{-1}$ , Figure 5a], and in Mg-talc [ $\delta(\text{Mg}_3\text{OH})$  at 669  $\text{cm}^{-1}$ ] (Russell *et al.*, 1970). In dioctahedral or trioctahedral minerals in which octahedral substitutions exist, the hydroxyl deformation band is generally in the region 700–950  $\text{cm}^{-1}$ . Its precise position is indicative of the nature of the species in the octahedral layer (Farmer, 1974). Thus, in the dioctahedral clay, pyrophyllite,  $\delta(\text{Al}_2\text{OH})$  is at 910  $\text{cm}^{-1}$ , and in an iron-montmorillonite,  $\delta(\text{Al}_2\text{OH})$  is at 918  $\text{cm}^{-1}$  and  $\delta(\text{FeAlOH})$  is at 890  $\text{cm}^{-1}$  (Farmer, 1979). In NaCo-smectite, this region was partially obscured by the strong, broad  $\nu(\text{SiO})$  band centered at 990  $\text{cm}^{-1}$ ; however, a shoulder was noted at about 905  $\text{cm}^{-1}$  (Figure 5b). In the acid-treated

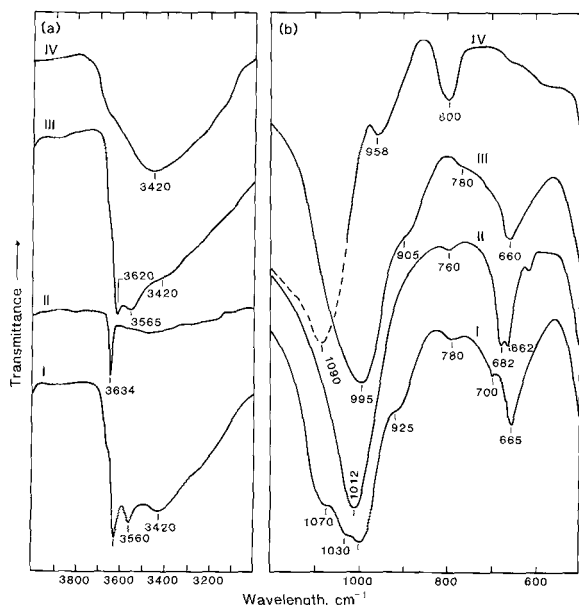


Figure 4. Infrared spectra of cobalt clays in (a) OH-stretching and (b) OH-deformation regions. I = acid-washed NaCo-smectite; II = cobalt talc; III = NaCo-smectite; IV = silica gel derived from exhaustive acid washing of NaCo-smectite to remove all of the cobalt.

smectite, a corresponding band at  $925\text{ cm}^{-1}$  was pronounced. This band is probably due to an OH-deformation mode  $\delta(\text{Co}_2\text{OH})$  arising from vacancies in the octahedral sheet. It is less likely due to a  $\nu(\text{Si}-\text{O})$  band of an SiOH group (*cf.*  $\nu(\text{Si}-\text{OH})$  in opal at  $965\text{ cm}^{-1}$  and in freshly precipitated silica gel at  $950\text{ cm}^{-1}$ ; Farmer, 1974). Indeed complete extraction of Co from NaCo-smectite by concentrated acid produced a white, noncrystalline silica gel (by X-ray and electron diffraction), still displaying a hexagonal, plate-like morphology and a  $\nu(\text{Si}-\text{OH})$  band at  $958\text{ cm}^{-1}$ . Finally, the band at  $684\text{ cm}^{-1}$  in Co-talc is presumably the  $a_1^2$  lattice mode of the silica sheets (Russell *et al.*, 1970).

**X-ray photoelectron spectra.** The main use of XPS in this study was to determine compositions; however, some information about the chemical state of the cobalt was obtained from the spectra. The XPS binding energy (B.E.) and Auger values for NaCo-smectite are B.E.  $\text{Co}2p_{3/2} = 781.0$ ,  $\Delta\text{B.E.}(2p_{1/2} - 2p_{3/2}) = 16.0$   $\Delta\text{B.E.} - (2p_{3/2}\text{-shake-up satellite}) = 5.1\text{ eV}$ , and  $\text{Co}(L_3VV)$  Auger kinetic energy =  $770.5\text{ eV}$ , whilst the corresponding values for Co-talc are  $781.1$ ,  $16.0$ ,  $5.6$ , and  $771.9\text{ eV}$ , respectively. The presence of a "shake-up" satellite structure and a  $\text{Co}2p_{1/2} - \text{Co}2p_{3/2}$  splitting of  $16.0\text{ eV}$  is indicative of high spin  $\text{Co}^{2+}$  (Dillard *et al.*, 1983); however, such parameters are not particularly sensitive to the metal coordination geometry. The shake-up satellite structure is generally due to ligand-to-metal charge transfer (Brisk and Baker, 1975). Separation of this line from the parent photoelectron

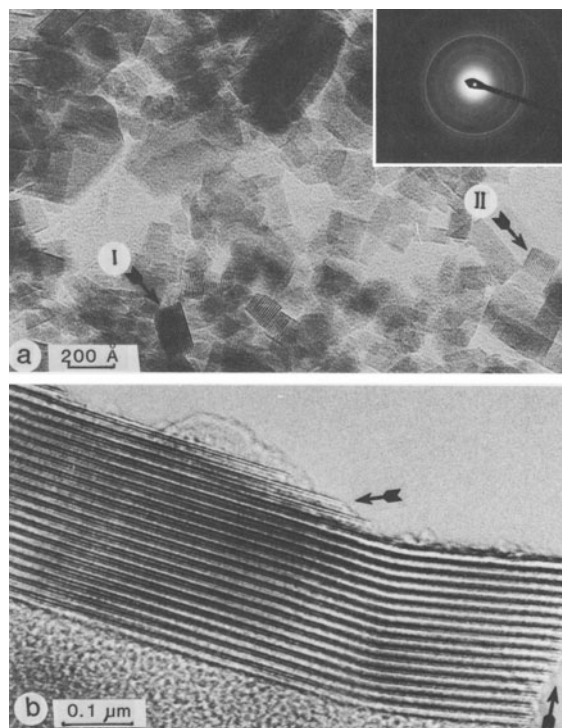


Figure 5. Transmission electron micrographs and diffraction pattern of the Co-deficient mica analyzing as  $\text{KCo}_{2.5}\text{Si}_4\text{O}_{10}(\text{OH})_2$ . (a) Low magnification shows short hexagonal blocks, some projected in  $[001]$  and others in  $[hk0]$ . As illustrated by I and II (arrowed), the relative dimensions in these directions vary considerably. (b) High resolution lattice image in  $[hk0]$  projection exhibits a greater regularity in lamellar order than found in the smectite shown in Figure 2b. Some structure is visible within the layers (arrowed).

line was greater in Co-talc than in NaCo-smectite. Inasmuch as the Co-O bonding in both materials is of similar covalency, this difference was presumably a measure of the increased ligand field splitting in Co-talc compared with the smectite, as can also be seen from the electronic spectra shown in Figure 3. These values are similar to those found for ionic cobalt adsorbed on chlorite ( $5.2\text{ eV}$ ) and for  $\text{Co}(\text{OH})_2$  ( $5.1\text{ eV}$ ) (Koppelman and Dillard, 1979; Sexton *et al.*, 1985).

#### Syntheses in presence of other cations

**Lithium.** Under conditions which are optimal for the formation of NaCo-smectite, slurries derived from cobalt nitrate, colloidal silica, and lithium hydroxide ( $\text{Co}:\text{Si}:\text{Li} = 2.5:4:12$ ) produced a mixture of two highly crystalline, bright-blue phases upon hydrothermal treatment. The XRD patterns of these phases, neither of which was clay-like, were identical to those reported by West and Glasser (1972) as the  $\beta_{11}$  and  $\gamma_{11}$  polymorphs of  $\text{Li}_2\text{CoSiO}_4$ .

**Potassium.** Potassium hydroxide slurries of the stoichiometry  $\text{Co}:\text{Si}:\text{OH} = 2.5:4:12$  produced a relatively

Table 5. X-ray powder diffraction data for K- and Cs-clays and Co-chrysotile.

| Index<br>( <i>hkl</i> ) <sup>1</sup> | KCo-mica (Co-rich)<br>d (Å) (I) <sup>3</sup> | KCo-mica <sup>2</sup> (Si-rich)<br>d (Å) (I/I <sub>0</sub> ) | CsCo-vermiculite<br>d (Å) (I) <sup>3</sup> | CsCo-mica<br>d (Å) (I) <sup>3</sup> | Co-chrysotile<br>d (Å) (I) <sup>3</sup> |
|--------------------------------------|--|--|--|-------------------------------------|---|
| 001 <sup>2</sup>                     | 10.6   | 10.2 (100)   | 11.0                                       | 11.0                                | 7.6 (s)                                 |
| 002 <sup>2</sup>                     |  | 5.05 (3)   | 5.42                                       |                                     | 4.65 (m)                                |
| 02,11                                | 4.71 (m)                                     | 4.56 (8)   | 4.61 (m)                                   | 4.74 (m)                            | 3.79 (w)                                |
| 003                                  |  | 3.40 (20)  |  |                                     | 2.70 (s)                                |
| 13,20                                | 2.69 (s)                                     | 2.63 (12)  | 2.62 (s)                                   | 2.69 (vs)                           | 1.58 (w)                                |
|                                      |  | 2.56 (8)   | 2.48 (m)                                   | 2.50 (m)                            | 1.34 (s)                                |
|                                      | 2.48   | 2.44 (5)   | 2.34 (m)                                   | 2.37 (s)                            |   |
| 04,22                                | 2.23 (m, br)                                 | 2.28 (5)   | 2.26 (m, br)                               | 2.26 (w)                            |   |
|                                      |  | 2.18 (2)   |  |                                     |   |
| 005                                  |  | 2.03 (1)   |  |                                     |   |
| 15,24,31                             | 1.76 (w)                                     | 1.70 (3)   | 1.74 (w)                                   | 1.74 (w)                            |   |
|                                      | 1.548  | 1.539 (8)  | 1.551                                      |                                     |   |
| 06,33 <sup>2</sup>                   | 1.538  | 1.524 (5)  | 1.542                                      | 1.547 (br)                          |   |
| 26,40                                | 1.352 (m)                                    | 1.336 (5)  | 1.323 (m)                                  | 1.335 (m)                           |   |

<sup>1</sup> 00*l* or *hk* index for a 2:1 layer silicate.

<sup>2</sup> From X-ray powder pattern, otherwise from electron diffraction from polycrystalline sample.

<sup>3</sup> s = strong, m = medium, w = weak, br = broad.

pure, deep-blue clay-like phase, whose XRD pattern exhibited a basal reflection at 10.2 Å (wet) and 060, 330 spacings typical of a trioctahedral clay (Table 5). Well-ordered stacks, as thick as fifty layers, were evident in electron micrographs (Figure 5a). This material did not swell in various glycols, which suggests a higher layer charge than the sodium analogue (Walker, 1961). Chemical analysis by XPS gave a composition consistent with a mica,  $\text{KCo}_{2.5}\square_{0.5}\text{Si}_4\text{O}_{10}(\text{OH})_2$ , in which the layer charge apparently arises from octahedral vacancies. A magnesium analogue  $\text{KMg}_{2.5}\square_{0.5}\text{Si}_4\text{O}_{10}(\text{OH})_2$ , with a structure intermediate between di- and trioctahedral, was reported by Seifert and Schreyer (1965, 1971) and by Kwak (1971). The intense blue color of the KCo-mica [ $\nu_{\text{max}}$  18,100(sh), 16,800(sh), 15,600  $\text{cm}^{-1}$ ] is similar to that of the NaCo-smectite, indicating the presence of some tetrahedral cobalt.

If the reactant stoichiometry was adjusted to be Si deficient (Co:Si:K = 3:2:12), hydrothermal treatment at 250°C under hydrogen produced a blue, flocculent, less crystalline cobalt clay phase together with a minor amount of a denser and more crystalline clay phase. An excess of cobalt yielded a mixture of  $\alpha$ - and  $\beta$ -Co(OH)<sub>2</sub>. The two clay phases were largely separable by decantation. TEM of the flocculent major product (Figure 6) revealed thin, irregular, hexagonal plates, together with small amounts of the minor phase, which appeared to be similar to that shown in Figure 5. The flocculent phase did not swell in ethylene glycol and showed a basal spacing of 10.6 Å (wet) and an 06 reflection indicative of a trioctahedral clay mineral (Table 5). Elemental analysis indicated that this material is also a mica but with a formula  $\text{KCo}_3\text{Si}_{3.75}\square_{0.25}\text{O}_{10}(\text{OH})_2$ , in which the layer charge apparently results from a deficiency of silicon rather than cobalt.

*Cesium*. Silica-deficient slurries derived from cesium hydroxide (Co:Si:OH = 3:2:10) produced a non-swelling, blue clay with a basal spacing of 10.7 Å and the 06 value expected for a trioctahedral clay mineral (Table 5). The excess cobalt appeared as  $\beta$ -Co(OH)<sub>2</sub>. A TEM of the clay fraction showed it to possess an unusual annular habit (Figure 7a). Chemical analysis by XPS indicated a considerable deficiency in silicon with the consequent layer charge apparently compensated for by cesium. The cation composition, corresponding to  $\text{Cs}_{1.34}\text{Co}_{3.03}\text{Si}_{3.65}\square_{0.35}\text{O}_{10}(\text{OH})_2$ , suggests that this phase is intermediate between a mica and a brittle mica. At a similar stoichiometry, the corresponding Na system yielded a smectite. At higher silica concentrations (Co:Si:Cs = 2.5:4:12), essentially a single, blue clay phase was produced which also had an annular,

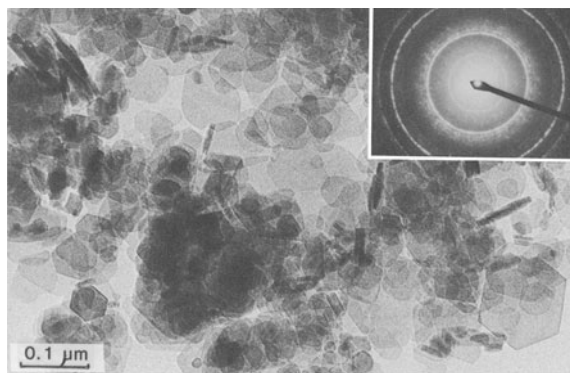


Figure 6. Transmission electron micrograph and diffraction pattern of the silica-deficient mica,  $\text{KCo}_3\text{Si}_{3.75}\text{O}_{10}(\text{OH})_2$ . Although plates have a distinct hexagonal morphology, their stacking is more disordered than that found in the Co-deficient mica (Figure 5). Well-defined blocks are absent.



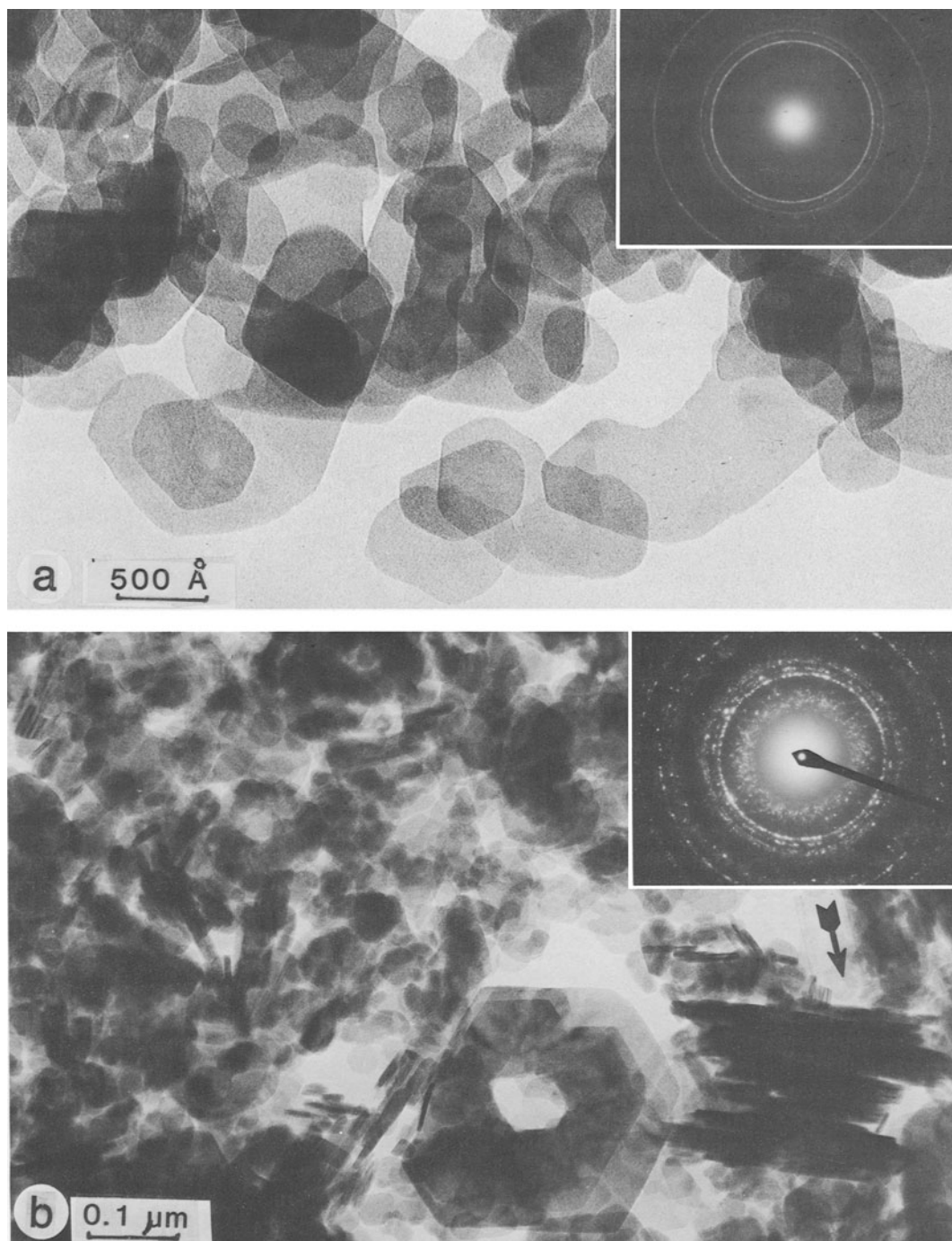


Figure 7. Transmission electron micrograph and diffraction pattern of (a) Cs-mica,  $\text{Cs}_{1.3}\text{Co}_3\text{Si}_{3.65}\text{O}_{10}(\text{OH})_2$  and (b) Cs-vermiculite,  $\text{Cs}_{0.7}\text{Co}_{3.2}\text{Si}_{3.7}\text{O}_{10}(\text{OH})_2$ . These crystals adopt a partial or complete annular morphology probably due to changes in the director of growth in the  $(hk)$  plane. Vermiculite plates occur as irregularly shaped books (arrow).

hexagonal, plate-like morphology (Figure 7b) and did not swell in ethylene glycol. This material is termed a vermiculite on the basis of the cation analysis by XPS which gave the composition,  $\text{Cs}_{0.70}\text{Co}_{3.23}\text{Si}_{3.71}\square_{0.29}\text{O}_{10}(\text{OH})_2$ . The characteristic blue color of these Cs-clays

here also suggests that some tetrahedral cobalt was present in the structure.

*Tetraalkylammonium.* With tetraalkylammonium hydroxides,  $\text{NR}_4^+ \text{OH}^-$  (R = methyl, ethyl, or n-propyl),

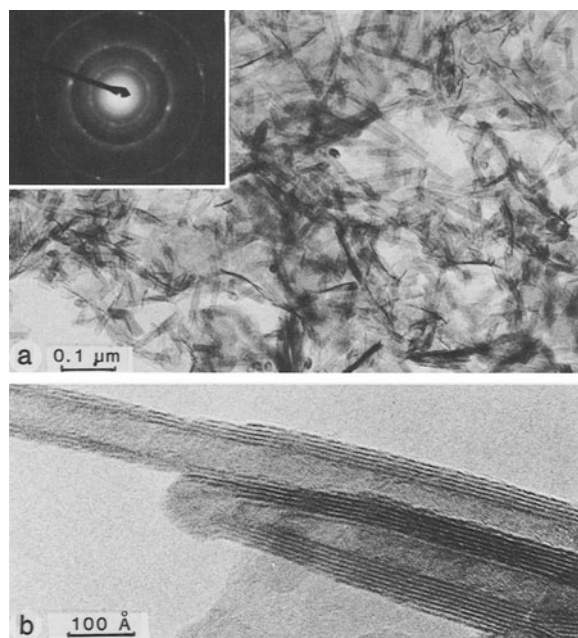


Figure 8. Transmission electron micrographs and diffraction pattern of Co-chrysotile: (a) Low magnification image shows tubes typically 0.1–0.2- $\mu\text{m}$  length and 100–200 Å in diameter. Sample is contaminated with a small amount of a “crumpled foil” phase. (b) Tube walls consist of layers with varying thickness; the tubes taper towards their ends as the number of layers decreases.

slurries in the ratio  $\text{Co}:\text{Si}:\text{NR}_4^+ = 3:2:5$  produced mainly pink Co-chrysotile [ $\nu_{\text{max}}$  23,500(sh), 20,800, 17,200(sh)  $\text{cm}^{-1}$ ]. As can be seen in Figure 8, the fibers display a fragmented tubular morphology. The XRD and SAD patterns were both diffuse (Table 5). A similar morphology was reported for Co-chrysotile by Noll *et al.* (1960). Analytical data indicated the product to be somewhat Co-deficient and Si-rich. At ratios which produced monophasic NaCo-smectite with NaOH, tetramethylammonium hydroxide slurries ( $\text{Co}:\text{Si}:\text{NMe}_4^+ = 2.5:4:12$ ) produced a mixture of products including both crumpled foils and ill-formed hexagonal plates [basal spacing = 14.1 Å (wet)]. The nature of these products has not been determined.

The addition of sodium ions to reaction mixtures which otherwise produced Co-chrysotile (i.e.,  $\text{Co}:\text{Si}:\text{NR}_4^+:\text{OH}:\text{NaCl} = 3:2:5:5$ ) resulted in a “crumpled foil” silicate product; no chrysotile was observed by electron microscopy. The “crumpled foil” phase was also produced by the addition of tetraethylammonium bromide to a mixture which should have favored the formation of NaCo-smectite ( $\text{Co}:\text{Si}:\text{NR}_4^+:\text{Br}:\text{NaOH} = 2.5:4:16:12$ ). At 350°C, a Co-talc was produced from these mixed cation reactions. In every run, the tetraalkylammonium ion was thermally unstable under the hydrothermal conditions employed, extensively degrading to

the free trialkylamine and various hydrocarbon products.

## DISCUSSION

### Structure of the NaCo-smectite

The XRD and electron diffraction data and the swelling behavior of the NaCo-smectite indicate that it is indeed a smectite. Chemical analyses give a remarkably low formal layer charge for this clay ( $\sim 0.1$  per  $\text{O}_{10}(\text{OH})_2$  formula unit). We have been unable to find reports of natural smectites with comparable layer charge; however, the presence of interlayer water and the clay’s swelling properties clearly demonstrate that the material is not a talc. This material presents a problem concerning the stereochemistry and position of the cobalt ions, because it is clear from electronic spectra that some of the cobalt is in tetrahedral coordination. In view of the deep blue colors of the KCo-micas and the CsCo-clays, some tetrahedral cobalt must also be present in these products; however, the major portion of the cobalt has octahedral coordination. Although XRD data for NaCo-smectite [ $d(060) = 1.557$  Å] suggest a trioctahedral structure and the cobalt content of the material is even slightly greater than that expected for complete octahedral occupancy, some octahedral vacancies are probably present, consistent with the assigned  $\delta(\text{Co}_2\text{OH})$  mode in the IR spectrum. In addition, analyses suggest a slight deficiency of Si in the tetrahedral sheets. Cobalt in excess of that found in the octahedral sheets could be located in one or more of the following positions:

(1) As an ionic  $\text{Si}^{4+} \leftrightarrow \text{Co}^{2+}$  substitution in tetrahedral layers. Although the ionic radius of tetrahedral, high-spin  $\text{Co}^{2+}$  (0.574 Å) (Shannon, 1976) is substantially greater than that of  $\text{Si}^{4+}$  (0.26 Å),  $\text{Co}^{2+}$  may well substitute into the tetrahedral sheets, as  $\text{Fe}^{3+}$  (0.49 Å) commonly does in 2:1 layer silicates; substitution by  $\text{Co}^{3+}$  can be discounted as it does not adopt tetrahedral geometry. Similar substitutions of  $\text{Si}^{4+}$  by  $\text{Mg}^{2+}$  (0.57 Å) have been proposed by Kwak (1971), Seifert and Schreyer (1971), and by Tateyama *et al.* (1974, 1976) to rationalize the composition of magnesium-rich but silicon-deficient micas.

(2) As adsorbed hydroxy-cobalt species on edges or faces of the clay particles. The small particle size of NaCo-smectite (Figure 1a) would result in a relatively high surface area available for such adsorption.

(3) In the interlayer as a hydroxy-cobalt species. The possibility of some of the excess of cobalt being present as cations in the interlayer space may be excluded, because boiling the material with  $\text{Mg}(\text{NO}_3)_2$  solution (3.6 M) did not exchange any  $[\text{Co}(\text{H}_2\text{O})_6]^{2+}$  into solution. This procedure, however, might not have removed interlayer cobalt if it was present as a neutral tetrahedral hydroxy-cobalt species. Under such circumstances, such species must be present in randomly

disordered and isolated sites because no evidence was found for increased spacings in the XRD patterns. Similarly, high-resolution TEM showed lamellar lattice images with uniform spacing.

(4) In the hexagonal holes of the silica sheets. In such positions, cobalt could adopt a distorted tetrahedral coordination sphere by interaction with three framework oxygen atoms of the silica sheet and the hydroxyl of the octahedral sheet. From IR data Calvet and Prost (1971) suggested that the non-exchangeable lithium, formed from Li-montmorillonite on heating, is in hexagonal cavities. Russell and Farmer (1964) also showed (1964) that on heating, the interlayer cations of both  $\text{Li}^+$ - and  $\text{Mg}^{2+}$ -montmorillonites, were exchanged with protons, possibly those in the structure. In addition, replacement of the protons of the brucitic sheet with  $\text{Co}^{2+}$  during the formation of NaCo-smectite would result in a partial internal cancellation of the overall negative layer charge, thereby explaining the low net charge observed. We were unable, however, to induce cobalt to adopt a tetrahedral stereochemistry by cation exchange into pre-formed Na-montmorillonite (Wyoming bentonite) by simple aqueous exchange at temperatures as high as 250°C. Evidently tetrahedral cobalt is irreversibly positioned in the hexagonal cavities during the formation of the clay.

#### *Effect of alkali metal cation on product selectivity*

It is apparent that the nature of alkali metal cation in the starting materials played a crucial role in determining the nature and layer charge of the cobalt clay products. Although a much greater number of reactant ratios and conditions would be required to define the various stability fields, several trends are apparent:

(1) Alkali metal ions of a particular size were required to stabilize 2:1 phyllosilicate structures. In the absence of alkali metal ions, tetraalkylammonium hydroxides produced the 1:1 chrysotile structure. The metal ion apparently acted as a template for the formation of the 2:1 structure rather than the alkylammonium ions acting as a template for the formation of the 1:1 structure. This relationship is shown by our use of mixed alkylammonium/sodium hydroxide systems, which produced disordered structures resembling the 2:1 phase rather than chrysotile. Such results contrast with hydrothermal syntheses of zeolites in which the ammonium salt is generally considered to be the major template (Lok *et al.*, 1983). The absence of a strong template effect with the alkylammonium ions in the Co-clay synthesis may be due to the extensive thermal decomposition observed for these ions under conditions which are more severe than those used for zeolite synthesis.

(2) Small cations did not efficiently stabilize the 2:1 structure. Thus, non-clay-like orthosilicates were

formed exclusively with lithium and to a minor extent with sodium.

(3) Within limits, the ultimate magnitude of the layer charge is dependent upon the size of the alkali metal cation. Thus, sodium produced smectites, whereas cesium produced brittle mica. No explanation for this size effect can be given. The situation is complicated by the different hydration structures expected for the various cations (Slade *et al.*, 1985).

Two questions are thus still outstanding regarding these new cobalt layer silicates: (1) Which (if any) of the suggested alternative locations for tetrahedral cobalt is the correct one? (2) what effect does a particular alkali metal ion have in determining the nature of the products? Both of these matters require further experimental work.

#### ACKNOWLEDGMENTS

We thank H. McArthur for experimental assistance with some syntheses, D. Hay for performing the XRD and A. E. Hughes the XPS analyses. This work was partly funded by the National Energy Research, Development and Demonstration Program grant 82/2222.

#### REFERENCES

- Anderson, R. B. (1984) *The Fischer-Tropsch Synthesis*: Academic Press, Orlando, 122–129.
- Brindley, G. W., Bish, D. L., and Wan, H. M. (1979) Compositions, structures and properties of nickel-containing minerals in the kerolite-pimelite series: *Amer. Mineral.* **64**, 615–625.
- Brindley, G. W. and Brown, G. (1980) *Crystal Structures of Clay Minerals and their X-ray Identification*: Mineralogical Society, London, 169–180.
- Brisk, M. A. and Baker, A. D. (1975) Shake-up satellites in X-ray photoelectron spectroscopy: *J. Electron. Spect. Rel. Phenom.* **7**, 197–213.
- Bruce, L. A., McArthur, H., and Turney, T. W. (1984) Characterisation and evaluation of Fischer-Tropsch catalysts prepared hydrothermally: *Proc. 12th Aust. Chem. Eng. Conf., Melbourne, Australia*, 649–654.
- Calvet, R. and Prost, R. (1971) Cation migration into empty octahedral sites and surface properties of clays: *Clays & Clay Minerals* **19**, 175–186.
- Cotton, F. A., Goodgame, D. M. L., and Goodgame, M. (1961) The electronic structure of tetrahedral cobalt(II) complexes: *J. Amer. Chem. Soc.* **83**, 4690–4699.
- Dalmon, J.-A. and Martin, G.-A. (1968) Sur la préparation et la structure de silicates basiques de cobalt et de magnésium du type talc et antigorite: *C.R. Acad. Sci. Paris Série D* **267**, 610–613.
- Dalmon, J.-A., Martin, G.-A., and Imelik, B. (1973) Silicates basiques de cobalt: talc et antigorite: *J. Chim. Phys.* **70**, 214–224.
- Decarreau, A. (1981) Cristallogénèse à basse température de smectites trioctahédriques par vieillissement de coprecipités silicométalliques de formule  $(\text{Si}_{4-x}\text{Al}_x)\text{M}_3\text{O}_{11} \cdot n\text{H}_2\text{O}$ . *C.R. Acad. Sci. Paris Série II* **292**, 61–64.
- De Vynck, I. (1980) Synthèse de phyllosilicates de cobalt, de nickel, de cuivre et de zinc: *Silic. Industr.*, 51–66.
- Dillard, J. G., Schenk, C. V., and Koppelman, M. H. (1983) Surface chemistry of cobalt in calcined cobalt-kaolinite materials: *Clays & Clay Minerals* **31**, 69–72.

- Farmer, V. C. (1974) *Infra-red Spectra of Minerals*: Mineralogical Society, London, 331–364.
- Farmer, V. C. (1979) *Data Handbook for Clay Minerals and other Non-Metallic Minerals*: H. van Olphen and J. J. Fripiat, eds., Pergamon Press, Oxford, 285–338.
- Feitnecht, W. and Berger, A. (1942) Über die Bildung eines Nickel- und Kobaltsilicates mit Schichtergitter: *Helv. Chim. Acta* **25**, 1543–1547.
- Fergusson, J. (1970) Spectroscopy of 3d complexes: *Prog. Inorg. Chem.* **12**, 159–293.
- Gier, T. E., Cox, N. L., and Young, M. S. (1964) The hydrothermal synthesis of sodium amphiboles: *Inorg. Chem.* **3**, 1001–1004.
- Hazen, R. M. and Wones, D. R. (1972) Effect of cation substitutions on the physical properties of trioctahedral micas: *Amer. Mineral.* **57**, 103–129.
- Hewitt, D. A. and Wones, D. R. (1975) Physical properties of some synthetic Fe-Mg-Al trioctahedral biotites: *Amer. Mineral.* **60**, 854–862.
- Koppelman, M. H. and Dillard, J. G. (1979) The application of XPS to the study of mineral surface chemistry: *Proc. Int. Clay Conf., Oxford, 1978*, M. M. Mortland and V. C. Farmer, eds., Elsevier, Amsterdam, 153–166.
- Kwak, T. A. P. (1971) An experimental study on Fe-Mg micas transitional between dioctahedral and trioctahedral compositions: *Neues Jahrb. Miner. Monatsh.*, 326–335.
- Lok, B. M., Cannan, T. R., and Messina, C. A. (1983) The role of organic molecules in molecular sieve synthesis: *Zeolites*, 282–291.
- Longuet, J. (1947) Synthèse de silicates de nickel, magnésium et cobalt, présentant des structures du type kaolinite-antigorite: *C.R. Acad. Paris Série D* **225**, 869–872.
- Nesterchuk, N. I., Makarova, T. A., and Fedoseev, A. D. (1968) Hydrothermal synthesis of a fibrous Na-Co amphibole: *Dokl. Akad. Nauk S.S.S.R. (English Transl.)* **179**, 201–202.
- Noll, W., Kircher, H., and Sybertz, W. (1960) Über synthetischen Kobaltchrysotil und seine Beziehungen zu anderen Solenosilikaten: *Beitr. Mineral. Petr.* **7**, 232–241.
- Pistorius, C. W. F. T. (1963) Some phase relations in the systems CoO–SiO<sub>2</sub>–H<sub>2</sub>O, NiO–SiO<sub>2</sub>–H<sub>2</sub>O and ZnO–SiO<sub>2</sub>–H<sub>2</sub>O to high pressures and temperatures: *Neues Jahrb. Mineral. Monatsh.* **2-3**, 30–57.
- Russell, J. D. and Farmer, V. C. (1964) Infrared spectroscopic study of the dehydration of montmorillonite and saponite: *Clay Min. Bull.* **5**, 443–464.
- Russell, J. D., Farmer, V. C., and Velde, B. (1970) Replacement of OH by OD in layer silicates, and identification of the vibrations of those groups in infra-red spectra: *Mineral. Mag.* **37**, 869–879.
- Seifert, F. and Schreyer, W. (1965) Synthesis of a new mica, KMg<sub>2.5</sub>[Si<sub>4</sub>O<sub>10</sub>](OH)<sub>2</sub>: *Amer. Mineral.* **50**, 1114–1118.
- Seifert, F. and Schreyer, W. (1971) Synthesis and stability of micas in the system K<sub>2</sub>O–MgO–SiO<sub>2</sub>–H<sub>2</sub>O and their relations to phlogopite: *Contr. Mineral. Petrol.* **30**, 196–215.
- Sexton, B. A., Hughes, A. E., and Turney, T. W. (1985) An XPS and TPR study of the reduction of promoted cobalt-kieselguhr Fischer-Tropsch catalysts: *J. Catalysis* (in press).
- Shannon, R. D. (1976) Revised effective ionic radii and systematic studies of interatomic distances in halides and chalcogenides: *Acta Crystallogr.* **32A**, 751–767.
- Slade, P. G., Stone, P. A., and Radoslovich, E. W. (1985) Interlayer structures of the two-layer hydrates of Na- and Ca-vermiculites: *Clays & Clay Minerals* **33**, 51–61.
- Tateyama, H., Shimoda, S., and Sudo, T. (1974) The crystal structure of synthetic Mg<sup>iv</sup> mica: *Z. Kristallogr.* **139**, 196–206.
- Tateyama, H., Shimoda, S., and Sudo, T. (1976) Infra-red absorption spectra of synthetic Al-free magnesium micas: *Neues Jahrb. Mineral. Monatsh.*, 128–140.
- Walker, G. F. (1961) Vermiculite minerals: in *The X-ray Identification and Crystal Structures of Clay Minerals*, G. Brown, ed., Mineralogical Society, London, 297–324.
- West, A. R. and Glasser, F. P. (1972) Preparation and crystal chemistry of some tetrahedral Li<sub>3</sub>PO<sub>4</sub>-type compounds: *J. Solid State Chem.* **4**, 20–28.

(Received 26 March 1985; accepted 7 October 1985; Ms. 1475)